High Throughput Screening of Library Compounds Against an Oligonucleotide Substructure of an RNA Target

Karen B. Gooding, Richard Higgs, Barry Hodge, Eric Stauffer, Beverly Heinz, Kevin McKnight, Krista Phipps, Michael Shapiro, Malcolm Winkler, Wai-Leung Ng, and Randall K. Julian
Eli Lilly and Company, Indianapolis, Indiana, USA

Approximately 300,000 compounds from selected libraries were screened against a subdomain of a hepatitis C viral (HCV) RNA using a high throughput flow injection mass spectrometry (FIA-MS) method with automated data storage and analysis. Samples contained 2 μM RNA target and 10 μM of each of up to ten ligands. Preliminary studies to optimize operational parameters used the binding of aminoglycosides to the A44 subdomain of bacterial RNA. Binding (confirmed by titration) and sensitivity were maximized within the constraints of the library and throughput. The mobile phase of 5 mM ammonium acetate in 50% isopropanol maintained the noncovalent complexes and provided good detection by electrospray mass spectrometry. Additionally, this composition maximized general solubility of the various classes of compounds including the oligonucleotide and organic library molecules. Cation adduction was insignificant in this screen although some solute and target dependent acetate adduction was observed. The ion trap mass spectrometer provided sufficient mass resolution to identify complexes of RNA with known components of the library. Converted mass spectral data (netCDF) were subjected to two types of statistical evaluation based on binding. The first algorithm identified noncovalent complexes that correlated with the molecular weights of the injected compounds. The second yielded the largest peak in the noncovalent complex region of the spectrum; this spectrum may or may not correlate with expected well components. Sixty-three compounds were confirmed to bind by more stringent secondary testing. Titrations, which were carried out with selected binding compounds, yielded a range of dissociation constants. Biological activity was observed for eleven confirmed binders. (J Am Soc Mass Spectrom 2004, 15, 884–892) © 2004 American Society for Mass Spectrometry

Detection of noncovalent complexes of biological macromolecular targets such as proteins [1] or nucleic acids [2] with drugs by mass spectrometry has become a valuable tool in drug discovery [3, 4]. Proteins or nucleic acids that will ionize and yield good mass spectra can be analyzed by direct methods, whereas those that are not amenable to mass spectrometry due to size or solubility require indirect methods [3]. Direct detection of noncovalent complexes can be accomplished by either electrospray ionization (ESI) or matrix assisted laser desorption ionization (MALDI). ESI has the advantage of compatibility with chromatographic injection methods and can thus be readily adapted for high-throughput screening. One requirement of the direct detection of noncovalent complexes by ESI is the ability of the target to ionize in its native state (conditions in which it binds ligands). Limitations are usually due to the size or structure of the target or the inability to remove cation adducts, a major problem for oligonucleotides which are polyanions. When the ionization is effective, and binding of ligands is retained throughout the process, ESI yields the molecular weight of the noncovalent complex and, therefore, the bound compound. Because ionization is primarily based on the macromolecule, the ionization characteristics of the ligand are relatively unimportant, thus providing a general screening method for a diverse library.

RNA is a validated drug target as substantiated by the use of erythromycin and aminoglycosides as antibacterial agents [5–7]. Functional domains of several RNA substructures have been shown to retain their binding capabilities during ESI/MS [2, 8]. Noncovalent complexes of oligonucleotides are formed in the presence of organic solvent and millimolar concentrations of salt, conditions which are compatible with flow injection mass spectrometry in the negative ion mode. Screening compound libraries against RNA targets has also been successfully undertaken [8, 9], as has determining structure-activity relationships (SAR) by mass spectrometry [8]. Most studies of noncovalent com-

Published online April 9, 2004
Address reprint requests to Dr. K. Gooding, Lilly Corporate Center, Eli Lilly and Co., Indianapolis, IN 46285, USA. E-mail: gooding_karen@lilly.com

1044-0305/04/$30.00
doi:10.1016/j.jasms.2004.02.010

Received November 3, 2003
Revised February 24, 2004
Accepted February 24, 2004

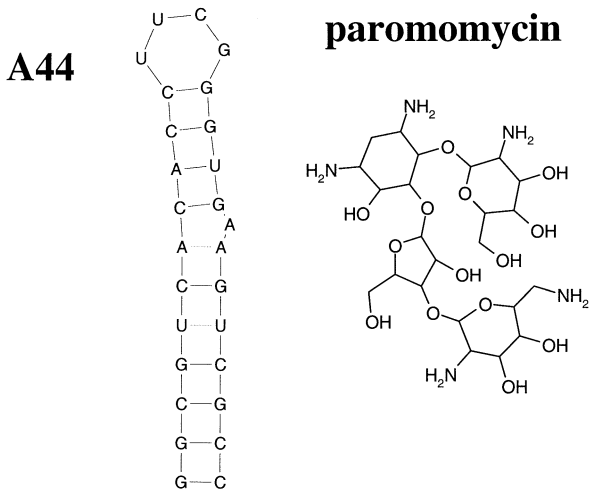

Figure 1. Structures of A44 subdomain of 16S RNA, the control bacterial target, and paromomycin, an aminoglycoside. Structures were drawn with RNAdraw [15].

plexes of RNA indicate that the gas-phase binding data correlate with those of the solution phase [2, 10].

One well-studied subdomain of 16S bacterial rRNA is the A44 domain. The binding of aminoglycoside antibiotics to A44 has been examined in detail using mass spectrometry in terms of both dissociation constants and binding sites [2, 11]. Figure 1 illustrates the structures of A44 and paromomycin, an aminoglycoside which has a dissociation constant of about 0.1 μM [12].

This paper describes the high-throughput screening (HTS) of approximately 300,000 compounds from selected libraries against a subdomain of Hepatitis *C* viral (HCV) RNA. Flow injection analysis (FIA) with detection by negative ion electrospray ionization mass spectrometry (ESI/MS) on an ion trap instrument provided a robust method to screen up to 10,000 compounds per day. The automated system included pooling of the potential ligands, mixing with target, high/low flow rates and data analysis, ultimately yielding ranked lists based on noncovalent binding to the target, peak correlation between the target and the complex, and signal intensities.

Experimental

Pooling

Library compounds from multiple libraries, 10 mM in dimethylsulfoxide (DMSO), were diluted and pooled to a final concentration of 11.4 μM each in 5 mM ammonium acetate in 50% isopropanol (<1% DMSO). A Tecan (Research Triangle Park, NC) Genesis Workstation 200 with CCS Packard (Torrance, CA) PlateStak plate stackers pooled up to ten ligands per well automatically using predefined pooling rules, bar coded plates and customized software described elsewhere [13].

Flow Injection-Mass Spectrometry

The pooled library compounds were mixed, one row at a time, with 5 μl RNA (20 μM in 50 mM ammonium acetate in 50% isopropanol) and then injected into eight 2 μl injection loops simultaneously using a Tecan robot. The final concentrations were 2 μM RNA and 10 μM ligand. Parallel sets of injection loops allowed adequate washing to occur. A programmable logic controller (PLC) controlled the timing of each injection (one every 30 s), and sent a contact closure signal to the mass spectrometer to begin each acquisition. After the acquisition of data for each row of samples, the raw files were converted to netCDF format and stored in a local database to allow easy retrieval and interpretation. The details of this process are described elsewhere [13]. The A44 subdomain of 16S rRNA (1 μM) was used as a control, bracketing each set of eight injections.

Shimadzu (Columbia, MD) LC10-AD HPLC pumps were controlled by a PLC for high and low flow rates. The timing was checked and adjusted daily, if necessary, to account for any slight changes in volume of the tubing. A ThermoFinnigan (San Jose, CA) LCQ Classic with a steel needle was used. The mobile phase was 5 mM ammonium acetate in 50% isopropanol. All reagents were HPLC grade.

RNA

The synthesized subdomains of RNA were obtained from Dharmacon Research, Inc. (Lafayette, CO) and Qiagen-Xeragon (Valencia, CA). The RNA was used as received if there was not excessive metal cation adduction in the mass spectrum. If cation adduction was high, the RNA was further purified by reversed phase solid phase extraction or HPLC using triethylamine as an ion-pairing agent to replace the metal.

Results and Discussion

RNA Targets

Feasibility studies and methods were developed with the A44 substructure of 16S RNA which has a molecular weight of 8635 Da. A44 is known to bind aminoglycosides such as paromomycin [6, 7]. Figure 1 illustrates the structures of this target and ligand pair. The target oligonucleotide in the high throughput screen described in this paper was SL-3e, a 14-mer substructure of Hepatitis *C* viral (HCV) RNA. It has a molecular weight of 4501 Da, and is shown in Figure 2. It was absolutely necessary that the oligonucleotides be pure and free of most metal cations to ensure that only one major ion would be observed by mass spectrometry. Metal cations were replaced with volatile cations by reversed phase solid phase extraction or HPLC.

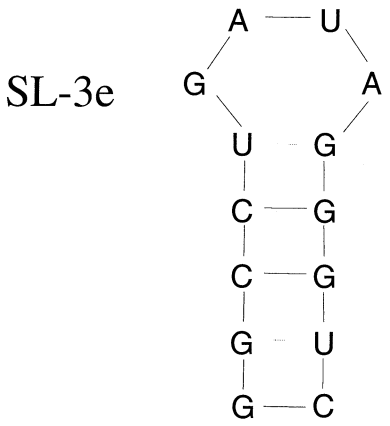

Figure 2. Structure of SL-3e subdomain of RNA [16]. Structure was drawn with RNAdraw [15].

Pooling

Compounds from several libraries, totaling almost 300,000, were pooled with up to ten per well using a novel clique-based algorithm to identify compatible sets of molecules based on reactivity rules and molecular weight overlap. Approximately 100 plates containing 88 wells of individual compounds were pooled each day into 13–15 destination plates. The library compounds were obtained in a DMSO solution and required dilution to a solution compatible with binding to the oligonucleotide target. A composition of 5 mM ammonium acetate in 50% isopropanol containing less than 1% DMSO yielded a good compromise for facilitating both complex formation and solubility of the RNA and library compounds. An aliquot of each well in the destination plate was mixed with the oligonucleotide target immediately before injection to produce final sample concentrations of 2 μM target and 10 μM of each ligand in 10 mM ammonium acetate in 50% isopropanol.

High Throughput Instrumentation

The general process and components of this high throughput system are diagrammed in Figure 3. The bar-coded plates allowed continuity of the process from pooling to data analysis. The design of the specialized injector and the software which controlled the processes are described in detail elsewhere [13].

Because the goal of this screen was a high throughput method, instrumental parameters were optimized to achieve a total analysis time of 30 s per injection. The prerequisite of the mobile phase was that it both preserve the integrity of the noncovalent complex and enhance detection by negative ion ESI. The suitability of the system using 5 mM ammonium acetate in 50% isopropanol was verified by the excellent spectral quality and preservation of the noncovalent A44-paromomycin complex seen in the spectra in Figure 4.

The injector was designed in-house to accommodate this high throughput method. It consisted of two parallel eight injector units which mixed the compounds of one row with target and then injected them simultaneously. The low dead-volume system resulted in only minimal additional band spreading to the flow injection peaks. The parallel design provided enough time to achieve thorough washing of the loops between samples. Carryover was occasionally observed due to the diverse sample set but it was minimized by the washing procedures with the mobile phase.

A high/low flow injection procedure was implemented to quickly move the sample to the ESI source at 200 μl/min, while providing washing of the tubing. During sample injection into the source, the flow was

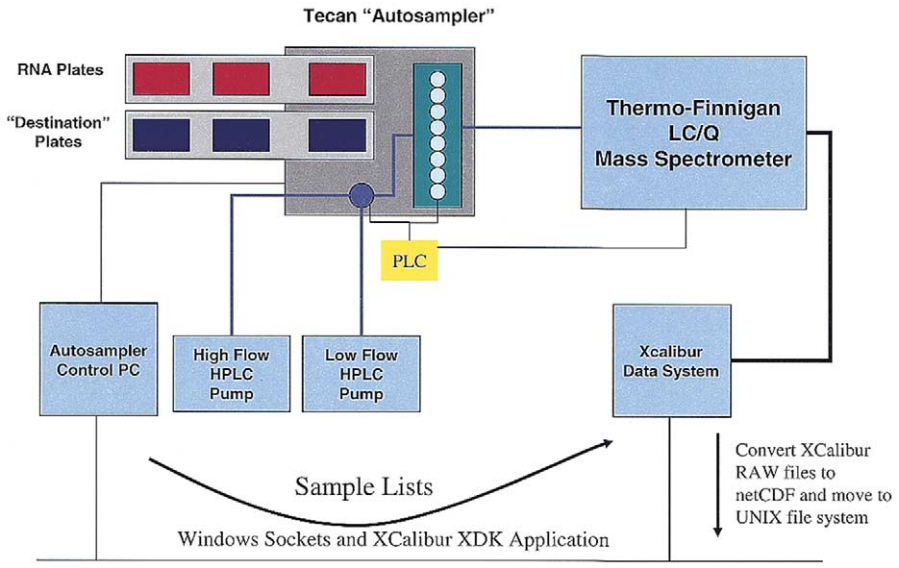

Figure 3. Design of the high throughput flow injection analysis-mass spectrometer system.

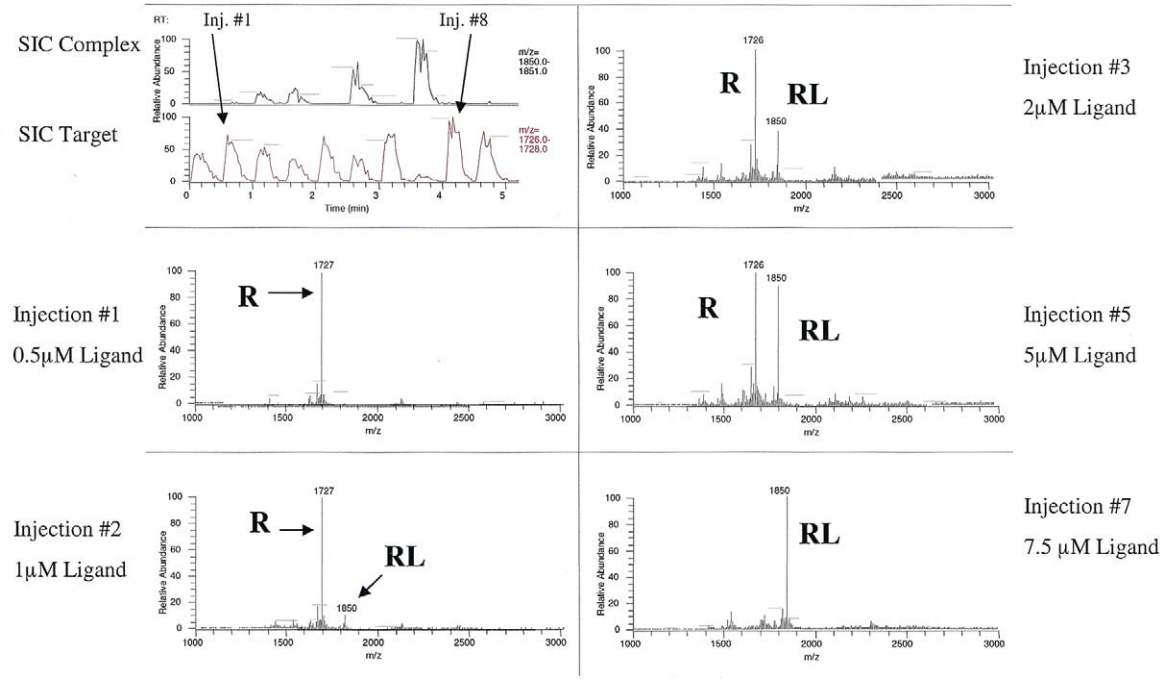

Figure 4. Titration of A44 (R) with paromomycin (L) using FIA with high/low flow. Upper left shows mass chromatogram of the A44/paromomycin complex (RL) at *m/z* 1850 and the mass chromatogram of the A44 target at *m/z* 1727. First and last peaks are bracketing control injections of A44 alone. At 0.5 μM paromomycin, shown at left center, the complex peak at *m/z* 1850 was not observed in the mass spectrum. At bottom left, the complex can be seen in injection no. 2 which included 1 μM paromomycin. The signal of the complex increased and the target signal decreased as the amount of paromomycin increased in injections no. 3, no. 5, and no. 7 as shown on the right.

reduced to 10 μl/min to provide a 15 s acquisition. The LCQ ion trap mass spectrometer was tuned at that low flow rate to maximize signal. Timing was checked daily and adjusted accordingly to compensate for small variations in system volume due to tubing expansion or blockage. The first and last injections of the 10 sample set were A44 controls to assess performance. The middle eight peaks were the injected samples.

Figure 4 illustrates a chromatogram and spectra of A44, the control oligonucleotide (*m/z* 1727), and its noncovalent complex with paromomycin (*m/z* 1850) during the lower levels of a titration. Each of the eight wells contained 2 μM A44. Wells 2, 3, 5, and 7 also contained 0.5, 1, 2, and 4 μM paromomycin, respectively. The upper mass chromatogram, corresponding to the noncovalent complex, showed an increase during titration, whereas the lower mass chromatogram of the target ions concomitantly decreased. By a concentration of 4 μM paromomycin, most of the target had been bound to the drug. Binding (B) was calculated by the areas of complex/(target + complex). Total binding would thus have a B value of 1. These data were used to generate the binding curve shown in Figure 5. The K_D obtained from the titration was 0.28 μM with a 95% confidence interval and is similar to dissociation constants obtained in other studies [9, 11]. Due to the limits of detection of this high throughput system, it was not possible to use levels of RNA below 2 μM which would have yielded more precise values of K_D [11]. At the 2 μM level, it was possible to detect noncovalent complex formation, identify the ligand if it was one of the well components, and obtain a general range of binding (i.e., $K_D < 10$ μM). The method was thus sufficient to classify the ligands as weak, strong or medium binders.

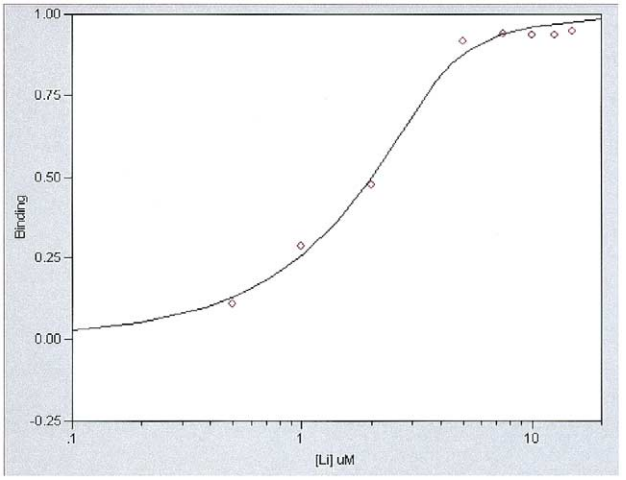

Figure 5. Titration curve generated by the noncovalent binding of A44 with paromomycin. $K_D = 0.28$ μM with a 95% confidence interval.

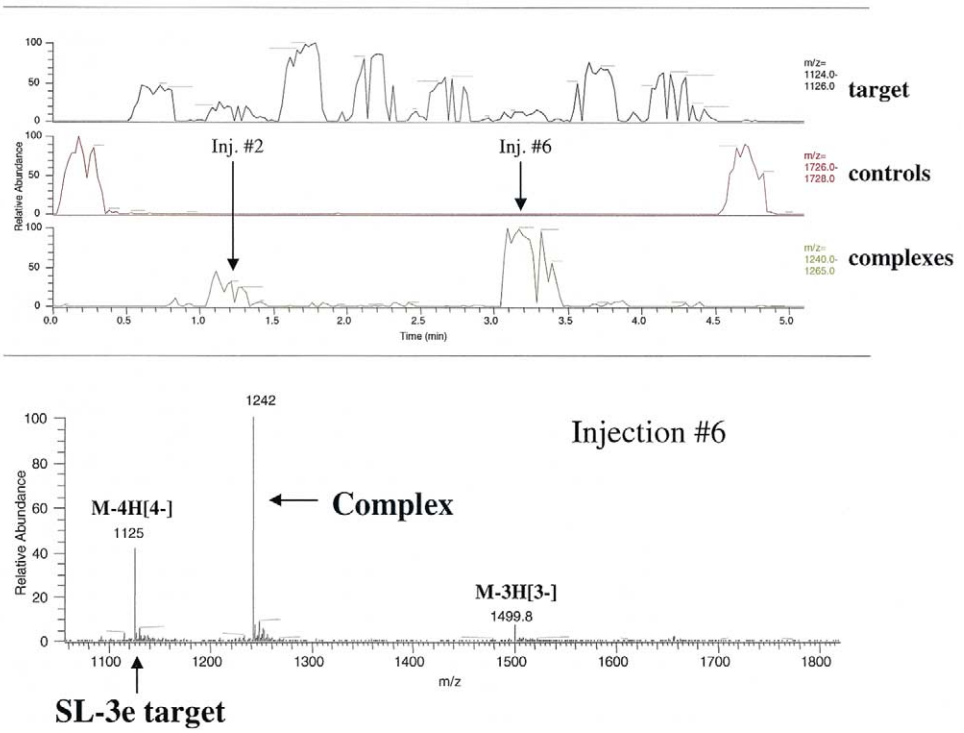

Figure 6. Noncovalent Binding of SL-3e with 2 ligands (injections no. 2 and no. 6). The mass chromatogram represents eight injections (plus two injections of controls) in the primary screen of the HCV target. Each injection contained the target and nine potential ligands. The summed mass spectra for injection no. 6 illustrates the formation of a noncovalent complex at *m/z* 1242.

MS Optimization

During method development, experimental design using JMP software (SAS Institute, Cary, NC) was used to expedite the optimization of the MS detection of noncovalent complexes of RNA with aminoglycosides. The experiments screened seven different factors in order to determine the main effects in the optimization. Those factors included capillary temperature, sheath gas flow rate, auxiliary gas flow rate, pH of the mobile phase, ESI voltage, mobile phase flow rate and the percentage of organic solvent in the mobile phase. The objective was to preserve the noncovalent complex and obtain the maximum absolute signal and minimal cation adduction. The main effects were caused by the sheath gas flow rate, the percentage of organic solvent, and the flow rate of the mobile phase. After optimization of these parameters, the instrument was tuned to maximize the oligonucleotide target signal using a combination of manual and automated tuning. The automatic gain control was turned off and a 200 ms injection time was employed. High-mass calibration was performed weekly using a sodium iodide solution and the vacuum level was monitored closely to obtain early warning of obstruction of the heated capillary. A sheath gas composed of oxygen/nitrogen [11] was used in preliminary studies but subsequent comparison with a sheath gas of 100% nitrogen demonstrated no advantage in detection of noncovalent complexes in this HTS FIA-MS method; consequently, 100% nitrogen was selected for convenience and cost.

The high-throughput FIA system had to operate unattended for approximately 18 h per day, four days per week. This requirement for a robust system prompted the replacement of the standard fused silica capillary tubing with a stainless steel needle kit to introduce samples into the ion trap. The large i.d. of the 32-gauge needle virtually eliminated plugging in the ESI source despite the inevitable introduction of samples that had limited or no solubility in the mobile phase. This substitution also eliminated the need for the occasional operator intervention required to correct slippage of the fused silica tubing in the spray needle. The 45 day screen had 97% uptime with routine maintenance being performed weekly.

Spectral Data

The spectra were generally of good quality with signal-to-noise ratio of at least 100 for 2 μM oligonucleotide. The SL-3e 14-mer target oligonucleotide of molecular weight 4502 produced both -3 and -4 charge states using this negative ion mass spectrometry procedure. Noncovalent complexes were usually observed in both charge states (Figure 6) but sometimes only the -4 charge state was formed. The mass chromatograms in Figure 6 show the SL-3e RNA target alone in the top portion, the

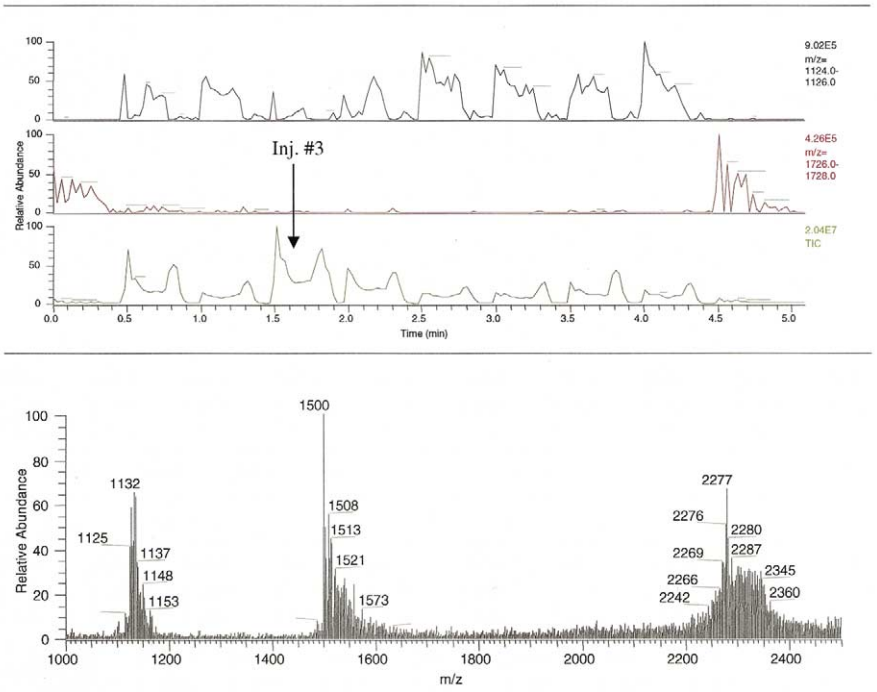

Figure 7. Mass chromatogram and spectrum of a highly adducted target. The total ion current chromatogram (TIC) in the lower trace is very high and the mass chromatogram for the target in the upper trace is very low for this injection (1.5–2.0 min).

A44 controls in the middle, and the noncovalent complexes in the bottom. It can be seen that a decrease in target was accompanied by an increase in complex in wells 2 and 6, which each contained a compound confirmed to bind to the target. Each of these wells additionally contained eight other compounds which did not form noncovalent complexes. The spectrum of injection 6 in the bottom panel very clearly indicates the complex peaks as well as the target, despite the presence of the eight other substances. The signal-to-noise ratio was greater than 100 in this example. No background subtraction or other data smoothing were done on the data.

Generally, little cation adduction was observed. Some samples, which were from diverse sources and contained varying amounts and composition of salts, produced significant adduction. This can be seen in the spectrum shown in Figure 7 from the third injection of the set (1.5–2.0 min). The salt sometimes increased the total ionization current and produced a significant −2 charge state peak, possibly indicating a concomitant pH change. This phenomenon usually resulted in a large TIC peak (bottom row) and decreased target (top row) due to the formation of an envelope of peaks instead of a discrete peak. When these samples were reanalyzed with a higher ammonium acetate concentration, the extensive adduction was either eliminated or greatly decreased. This may indicate a mixing or solubility problem during the primary HTS procedure or, more probably, replacement of the original cations with ammonium.

The other adduction which was commonly observed was that of acetate, as shown in Figure 8 for both the −3 and −4 charge states. Certain compounds and/or target RNA structures seemed to enhance this adduction. The FIA-MS procedure described in this report was used to analyze more than ten substructures of RNA of various molecular weights. The extent of acetic acid adduction was structure dependent when purified target was analyzed with the ammonium acetate/isopropanol mobile phase in solutions without any ligands. When collision induced dissociation was applied to the oligonucleotide-acetate complex, bond fragmentation occurred before loss of the acetate. Stable noncovalent anionic adducts of carbohydrates have been observed in other studies [14].

Data Acquisition and Analysis

The data files, which contained eight injections bracketed by controls, were acquired using Xcalibur software (ThermoFinnigan, San Jose, CA). Data were then transferred to a server and analyzed by a master program that identified peaks in the noncovalent complex region of the spectrum and their correlation with the known components of the well. Various attributes such as target and complex area under the curve (AUC), binding (B = complex/[target + complex]), and correlation of the elution of the noncovalent complex peak to that of the target were assessed and presented in a JMP database. The results could then be compared and complexes identified by man-

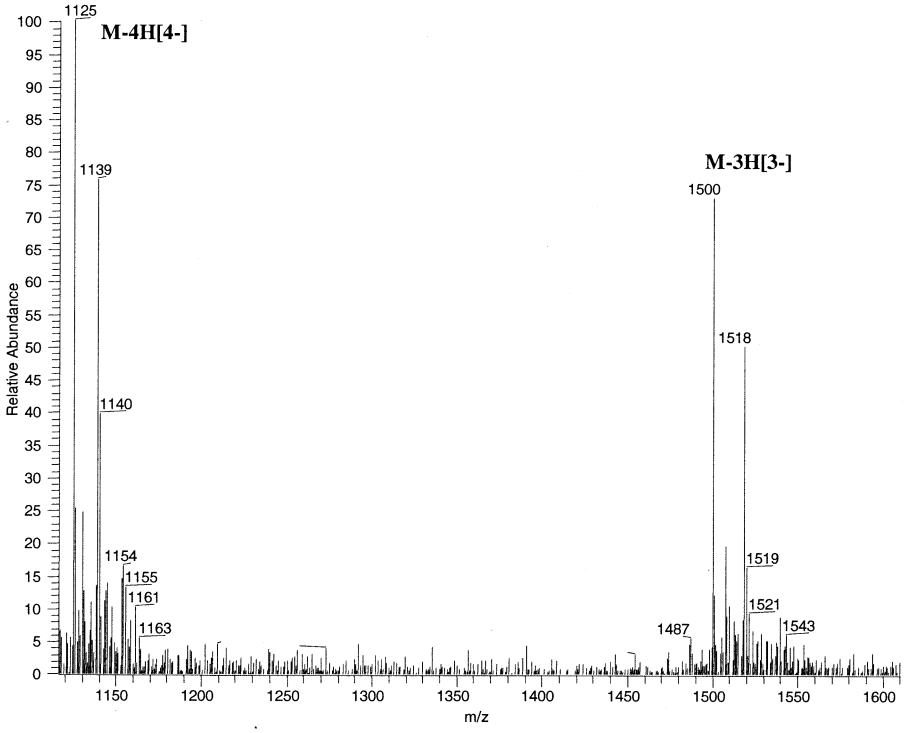

Figure 8. Acetate adduction of the SL-3e RNA subdomain. *m/z* 1125.1 is the −4 charge state.

ual inspection. Two databases were assembled. One was the *Ligand Lookup* table in which the binding and the AUC for every library component with target was assessed. The second was the *Ligand Scan* table in which only the highest peak in the noncovalent complex region of each injection was noted. In some cases, this was correlated with a noncovalent complex of a known component or an adduct thereof. In others, the peaks resulted from aggregated ligands or unknowns. Figure 9 shows the graphed data of each statistical analysis method for one batch of 14 destination plates pooled from about 10,000 compounds. Compounds which produced noncovalent complexes with significant binding and correlation were selected for confirmation by secondary testing.

The success of injections was assessed by the sum of the target and complex AUC to accommodate cases of either negligible or total binding. False positives were observed when substances associated as dimers or other aggregates. The diversity of the library included compounds of differing solubility in aqueous solvents; therefore, aggregation of some species in this or any

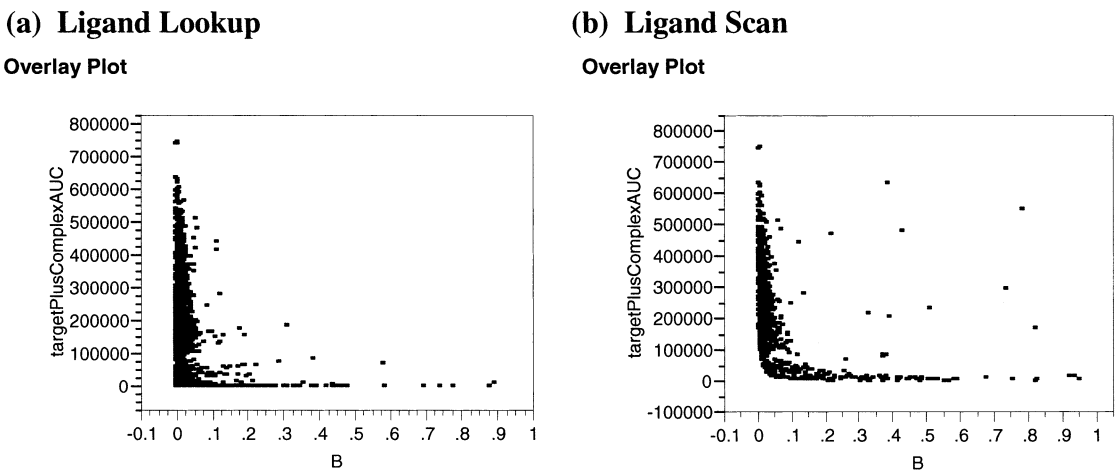

Figure 9. Statistical Presentation of Binding. The sum of target plus complex is plotted against binding (B). (**a**) *Ligand Lookup*: Correlated with ligand in the well. (**b**) *Ligand Scan*: Highest peak in injection (may or may not correlate with well contents).

Table 1. Ligands with biological activity

No.	Compound class	MS Binding		Biological assays IC_{50} IRES (μM)
		B (10 μM ligand)	K_D (μM)	
1	Peptide	0.30	10–50	3.3
2	Neutral	0.02	>100	3.76
3	Aminoglycoside	0.50	<10	4.4
4	Quaternary amine		weak	5.87
5	Quaternary amine	0.04	>100	7.37
6	Peptide	0.35	<10	7.8
7	Aminoglycoside	Plugged system		7.57
8	Quaternary amine	0.05	>100	10.87
9	Peptide	0.05	10–50	11.48
10	Aminoglycoside	0.60	<10	11.95
11	Peptide	0.30	10–50	12.6

mobile phase would be expected. Dimers frequently exhibited a sodium adduct as well as a single charge state which could be verified by acquiring higher resolution spectra (using the ZoomScan feature on the LCQ Classic) or by analyzing the sample on a Fourier transform ion cyclotron resonance spectrometer (FT-ICR). Secondary confirmation of binding delineated samples with a two step process which included high/low flow injection analysis of the possible ligand without and with the oligonucleotide, thus elucidating "ligands only" phenomena.

Secondary Confirmation of Binding

Compounds which appeared to form noncovalent complexes with the RNA substructure were reanalyzed without and with target on another FIA-MS system. This method implemented a single injection port and automatic mixing of the sample with target. High/low flow with the same mobile phase as in the primary screening resulted in similar spectra when binding did confirm. A higher salt concentration of 50 mM ammonium acetate in 50% isopropanol was used for the complex formation so that nonspecific interactions due to ionic forces would be minimized [8]. This was higher than the 10 mM salt in the sample in the primary HTS method.

A representative sampling of confirmed binders to include compounds from different classes of quaternary salts, aminoglycosides, peptides, and neutral molecules, were titrated against the target. They exhibited dissociation constants ranging from μM to mM binding. Biological activity was assayed on all compounds confirmed to form noncovalent complexes. Sixty-three compounds with B values greater than 0.1 in the primary screening were confirmed to bind in the secondary assay. Eleven of these, as listed in Table 1, exhibited biological activity. When the eleven active compounds were titrated to the target RNA substructure, three were strong binders ($K_D < 10$ μM), three were intermediate ($K_D = 10–50$ μM) and four were weak ($K_D > 100$ μM). The other compound was not totally soluble in the mobile phase and was not titrated to avoid plugging the system. Its B value of 0.44 in the primary HTS would suggest that it was also a tight binder. Only the confirmed binders with biological activity had K_D values indicating strong or intermediate binding. All biologically active compounds were titrated but only a representative number of the inactive ones were.

The spectral properties regarding charge state and multiple binding were also noted. Both charge states were usually observed. With the peptide ligands, however, only the −4 charge state was observed; these also tended to yield high acetic acid adducts. Due to these anomalies, peptide ligands were not generally detected by the *Ligand Lookup* data analysis program but were earmarked by the *Ligand Scan*. Most active ligands did not exhibit multiple binding to the target except at high levels during titration.

Conclusions

High throughput screening of library compounds against oligonucleotide targets was achieved with a flow injection analysis-negative ion mass spectrometry method. Ligands that formed noncovalent complexes were generally from the classes of compounds previously found to bind to RNA: Peptides, aminoglycosides, and cations [8]. Many other compounds in these classes were included in the library and did not form noticeable noncovalent complexes, showing selectivity for the method. The subset of compounds selected by the screen provided eleven compounds which also had biological activity and strong to intermediate binding characteristics. The screening method was robust, with 97% uptime.

References

1. Loo, J. A. Studying Noncovalent Protein Complexes by Electrospray Ionization Mass Spectrometry. *Mass Spectrom. Rev.* **1997,** *16,* 1–23.
2. Hofstadler, S. A.; Griffey, R. H. Analysis of Noncovalent Complexes of DNA and RNA by Mass Spectrometry. *Chem. Rev.* **2001,** *101,* 377–390.
3. Siegel, M. M. Early Drug Discovery Drug Screening Using Mass Spectrometry. *Curr. Top. Med. Chem.* **2002,** *2,* 13–33.
4. Hofstadler, S. A.; Griffey, R. H. Mass Spectrometry as a Drug Discovery Platform Against RNA Targets. *Curr Opin. Drug Discov.* **2000,** *3,* 423–431.
5. Gallego, J.; Varani, G. Targeting RNA with Small-Molecule Drugs: Therapeutic Promise and Chemical Challenges. *Acc. Chem. Res.* **2001,** *34,* 836–843.
6. Sucheck, S.; Wong, C.-H. RNA as a Target for Small Molecules. *Curr. Opin. Chem. Biol.* **2000,** *4,* 678–686.
7. Ecker, D.; Griffey, R. H. RNA as a Small-Molecule Drug Target: Doubling the Value of Genomics. *Drug Discov. Today* **1999,** *4,* 420–429.
8. Swayze, E. E.; Jefferson, E. A.; Sannes-Lowery, K. A.; Blyn, L. B.; Risen, L. M.; Arakawa, S.; Osgood, S. A.; Hofstadler, S.A.; Griffey, R. H. SAR by MS: A Ligand Based Technique for

Drug Lead Discovery Against Structured RNA Targets. *J. Med. Chem.* **2002,** *45,* 3816–3819.
9. Hofstadler, S. A.; Sannes-Lowery, K. A.; Crooke, S. T.; Ecker, D. J.; Sasmor, H.; Manalili, S.; Griffey, R. H. Multiplexed Screening of Neutral Mass-Tagged RNA Targets Against Ligand Libraries with Electrospray Ionization FTICR MS: A Paradigm for High-Throughput Affinity Screening. *Anal. Chem.* **1999,** *71,* 3436–3440.
10. Wang, F.; Freitas, M. A.; Marshall, A. G.; Sykes, B. D. Gas-Phase Memory of Solution-Phase Conformation: H/D Exchange and Fourier Transform Ion Cyclotron Resonance Mass Spectrometry of the N-Terminal Domain of Cardiac Troponin C. *Int. J. Mass Spectrom.* **1999,** *192,* 319.
11. Sannes-Lowery, K. A.; Griffey, R. H.; Hostadler, S. A. Measuring Dissociation Constants of RNA and Aminoglycoside Antibiotics by Electrospray Ionization Mass Spectrometry. *Anal. Biochem.* **2000,** *280,* 264–271.
12. Griffey, R. H.; Hofstadler, S. A.; Sannes-Lowery, K. A.; Ecker, D. J.; Crooke, S. T. Determinants of Aminoglycoside-Binding Specificity for rRNA by Using Mass Spectrometry. *Proc. Natl. Acad. Sci. U.S.A.* **1999,** *96,* 10129–10133.
13. Stauffer, E.; Hodge, B.; Julian, R., unpublished.
14. Cai, Y.; Concha, M. C.; Murray, J. S.; Cole, R. B. Evaluation of the Role of Multiple Hydrogen Bonding in Offering Stability to Negative Ion Adducts in Electrospray Mass Spectrometry. *J. Am. Soc. Mass Spectrom.* **2002,** *13,* 1360–1369.
15. Matzura, O.; Wennborg, A. RNA draw: An Integrated Program for RNA Secondary Structure Calculation and Analysis Under 32-bit Microsoft Windows. *CABIOS* **1996,** *12,* 247–249.
16. Lukavsky, P. J.; Otto, G. A.; Lancaster, A. M.; Sarnow, P.; Puglisi, J. D. Structures of Two RNA Domains Essential for Hepatitis C Virus Internal Ribosome Entry Site Function. *Nat. Struct. Biol.* **2000,** *7,* 1105–1110.